Supporting Information

Campàs et al. 10.1073/pnas.0911575107

SI Text

Beak Shape Digitization. Lateral photographs of museum specimens of each species were taken under both normal light exposure (Fig. 1*A*) and underexposed conditions (Fig. 1*B*). Underexposed photographs allow us to track the silhouette of the bird making the detection of the beak profile easier and more accurate. Using a feature detection program (Steerable—ImageJ plugin), we detect the contour of the beak at pixel resolution (Fig. 1*B*; Pixel size = 40 μm). The photograph taken under normal exposure allows the determination of the length axis of the beak, as traced in Fig. 1*A*. The beak profile obtained from the feature detection analysis corresponds to a set of points (pixels) in the plane (Fig. 1*C*—red dots). In order to obtain a smooth profile of the upper beak, we trace a Bezier spline of the upper contour of the beak (Fig. 1*C*—blue dots). The smooth upper beak profile obtained from the Bezier spline (Fig. 1*D*) is determined for all species and used for the pairwise comparison of shapes.

Pairwise Comparisons of Beak Shapes. Once the upper beak shapes for all species have been determined, we are interested in quantifying the differences between a given pair of shapes. Specifically, we want to quantify the difference between a reference, unmodified shape, and a beak shape transformed via a scaling transformation. To do so, we define the following metric distance between two real functions, $z_1(x)$ and $z_2(x)$:

$$\|z_1(x) - z_2(x)\| \equiv \frac{\int_0^{x_m} dx (z_1(x) - z_2(x))^2}{\int_0^{x_m} dx (z_1(x) + z_2(x))^2}, \qquad \text{[S1]}$$

where $x_m = \mathrm{Min}[x_1, x_2]$, with x_1 and x_2 being the maximal values that the x coordinates take for the functions $z_1(x)$ and $z_2(x)$ respectively. As explained in the main text, we define the error in the shape as $E_s(s_\ell, s_d) \equiv \|y_1(x) - T_{s_\ell s_d}[y_2(x)]\|$ which measures the difference between the undeformed shape $y_1(x)$ and the scaled version, $T_{s_\ell s_d}[y_2(x)]$, of a beak shape $y_2(x)$. The transformation $T_{s_\ell s_d}[\cdot]$ of the shape is implemented through the scaling matrix:

$$T_{s_\ell s_d} = \begin{pmatrix} s_\ell & 0 \\ 0 & s_d \end{pmatrix},$$

which is a particularly simple case of the general matrix representation of the affine group. In a similar way than for the shape, we define the error in the shape derivative as the quadratic difference between the derivatives of the reference and transformed shapes, i.e., $E_d(s_\ell, s_d) \equiv \|y_1'(x) - T_{s_\ell s_d}[y_2(x)]'\|$, where $y'(x) \equiv dy(x)/dx$ *. The defined measures are dimensionless quantities that depend only on the two scaling factors s_ℓ and s_d. A necessary condition for two given beak shapes to be related through a scaling transformation (meaning that they differ only in length and depth) is the existence of a minimum of both defined measures, E_s and E_d, for particular values s_ℓ^* and s_d^* of the scaling factors. The values of the measures at the minimum (the residuals, i.e., $E_s(s_\ell^*, s_d^*)$ and $E_d(s_\ell^*, s_d^*)$) measure how closely related the reference and transformed shapes are.

In order for the reference and transformed shapes to collapse, landmark points in one shape must be mapped onto the same landmark points of the other shape. In particular, the end point of the beak of the reference shape should coincide with the end point in the collapsed shape. This constrain allows us to estimate the scaling factors that may collapse the shapes. If the end points of the reference ($y_1(x)$) and compared ($y_2(x)$) shapes are given by (x_1, y_1) and (x_2, y_2) respectively (Fig. 2), then the scaling factors that may collapse the shapes must be close to

$$s_\ell = \frac{x_1}{x_2} \quad \text{and} \quad s_d = \frac{y_1}{y_2}. \qquad \text{[S2]}$$

The range of scaling factors within which one is allowed to search is determined by the experimental error in the measure of the end point of the beak, which is the major source of error in our experiments. If the coordinates of the end points of the beaks have experimental uncertainties δx_1, δx_2, δy_1 and δy_2 (Fig. 2), then the uncertainties in the scaling factors that may collapse the shapes are given by

$$\frac{\delta s_\ell}{s_\ell} = \sqrt{\left(\frac{\delta x_1}{x_1}\right)^2 + \left(\frac{\delta x_2}{x_2}\right)^2} \quad \text{and} \quad \frac{\delta s_d}{s_d} = \sqrt{\left(\frac{\delta y_1}{y_1}\right)^2 + \left(\frac{\delta y_2}{y_2}\right)^2}, \qquad \text{[S3]}$$

where the last expressions are obtained by error propagation in Eq. **2**. The experimental uncertainties in the coordinates, δx and δy, are the same for all shapes as they depend on the precision with which the last point is measured. From the thickness of the tip of the glass pipette we estimate $\delta y \simeq \delta x = 0.5$ mm. Therefore, the smaller the beak the larger the relative errors $\delta x/x$ and $\delta y/y$, leading to larger relative errors in the scaling factors (Eq. **3**). For simplicity, we consider an upper bound to the relative error in the determination of the end point of the beak: we approximate the relative error to be the same for all shapes and equal to that of the smallest beak, for which we estimate it to be $\delta x/x \simeq 0.05$ and $\delta y/y \simeq 0.05$, as the typical size of the smallest beaks (*C. olivacea* and *T. bicolor*) is about 10 mm. This is to say that the coordinates of the end point of the smallest beak are determined within a 5% precision (largest relative error). Using Eq. **3** we then estimate the relative error in the scaling factors to be

$$\frac{\delta s_\ell}{s_\ell} = \sqrt{2}\frac{\delta x}{x} \simeq 0.07 \quad \text{and} \quad \frac{\delta s_d}{s_d} = \sqrt{2}\frac{\delta y}{y} \simeq 0.07. \qquad \text{[S4]}$$

The range of scaling factors within which one is allowed to search for a minimum in E_s and E_d is thus $(s_\ell - \delta s_\ell, s_\ell + \delta s_\ell)$ and $(s_d - \delta s_d, s_d + \delta s_d)$. If no minima of E_s and E_d are found within this range, the shapes do not collapse under scaling transformations.

In the same way that the end point of the beak has an associated uncertainty, the direction of the length axis has an angular uncertainty $\delta\theta$ (Fig. 2), which arises from the uncertainty in the measurement of the point where the upper and lower beaks come together (Figs. 1, 2). If the coordinates of the point where the upper and lower beaks come together (as measured from the tip of the beak) are $(x_c, 0)$ and the uncertainty in the determination of this point is δy_c in the direction perpendicular to the length axis, then the angular uncertainty (for $\delta\theta \ll 1$) reads

$$\delta\theta = \frac{\delta y_c}{x_c}. \qquad \text{[S5]}$$

*We note that the best method to find out whether a reference and a transformed shape are indeed the same shape would be to show that these are congruent planar curves by comparing their local curvatures. Unfortunately, this method proved too noisy for our study.

The existence of an error in the determination of the direction of the length axis means that one has also to allow variations in the angle θ, which correspond to rotations of the compared shape $y_2(x)$ relative to $y_1(x)$. In the same way than previously done for the scaling factors, we determine the upper bound of the error in θ by considering the smallest beak and obtain $\delta\theta \simeq 0.12$ (approximately 7 degrees). We note that one does not know a priori what are the spatial directions along which the shape should be scaled. Therefore, regardless of the angular uncertainty $\delta\theta$, one should, in general, allow for rotations of the compared shape and ask if there exist values of the rotation angle θ and scaling factors s_ℓ and s_d that lead to a collapse of the shapes.

In Fig. 3 we compare the shapes of the Medium and Large Ground Finches (*Geospiza fortis* and *Geospiza magnirostris*). To find out if the shapes do collapse via a scaling transformation we minimize the measures E_s and E_d as a function of the scaling factors, and also as a function of the angle θ. Fig. 3*B*, *C* shows the existence of a minimum of both measures E_s and E_d as a function of θ, s_ℓ and s_d. The optimal relative rotation angle θ^* obtained by minimization is $\theta^* = 4 \pm 5$ degrees, which is consistent with the fact that the length axis and the axis perpendicular to length are the relevant axis for scaling, as the shapes collapse in this coordinate system (see below). At the optimal angle θ^*, there is a minimum of both measures as a function of the scaling factors (Fig. 3*B*); the obtained optimal scaling factors are $s_x^* = 0.67 \pm 0.01$ and $s_y^* = 0.51 \pm 0.07$, meaning that the shape of the upper beak of the Large Ground Finch must be reduced by about a 30% in length and 50% in depth in order to be superimposed on the shape of the upper beak of the Medium Ground Finch.

Measure of *Bmp4* Expression in the Beak Primordium. As explained in the main text, we analyze the *Bmp4* expression pattern in midsaggital sections of the frontonasal mass at embryonic stage 26 for specimens of the different species in the genus *Geospiza*. We defined four different measures of the expression pattern and correlated them with the scaling factors. In Fig. 4 we plot the expression levels of *Bmp4* as obtained using different measures, against the scaling factors. All measures (but measure 4) show a positive correlation of *Bmp4* expression and beak depth. Beak length also shows some degree of correlation with *Bmp4* expression, although to a lesser degree than for beak depth. Measure 4 quantifies the total area of mesenchymal *Bmp4* expression above 50% of the epithelial *Bmp4* levels, normalized to the total area of the beak; this measure shows essentially no correlation with beak length or depth. The measure of *Bmp4* expression that shows the best correlation with the scaling factors and, therefore, with adult beak morphology, is the maximal mesenchymal level of *Bmp4* relative to epithelial levels, as shown in the main text. When the maximal value of mesenchymal *Bmp4* expression is normalized to basal mesenchymal levels (away from the epithelium), similar results are obtained (Fig. 4), suggesting that the relevant magnitude is the maximal mesenchymal *Bmp4* expression level.

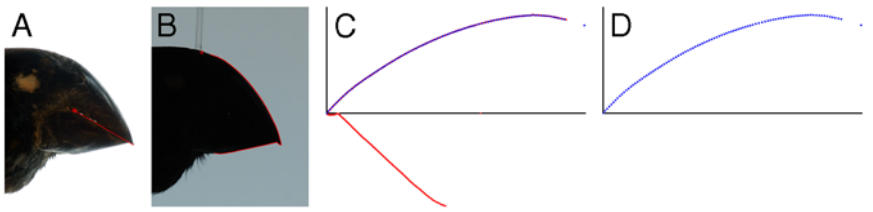

Fig. S1. Digitization of a beak profile. (*A*) Lateral photograph of a museum specimen of a male Large Ground Finch (*G. magnirostris*) under normal exposure conditions. The *red dot* corresponds to the position where upper and lower beaks come together, and the surrounding *red square* represents the associated experimental uncertainty in the determination of this point. The *red line*, traced from the tip of the beak to the specified *red dot*, specifies the axis of beak length. (*B*) Underexposed photograph of the same specimen as in A. The *red line* traces the profile of the beak and was determined using a feature detection software. The end point of the beak (*red dot*) corresponds to the position where the keratin layer ends and the associated *red square* represents the experimental uncertainty in the measurement of this point, which was determined with the help of a glass pipette (visible in the photograph). (*C*) Beak profile as obtained using a feature detection software (*red*) and Bezier spline of the upper beak profile (*blue*). (*D*) Upper beak profile used in the comparative analysis of beak shapes (same Bezier spline of the digitized beak profile as in C). In both C and D, the beak shape has been rotated so that the length axis of the beak corresponds to the *x* axis and the origin of coordinates is at the tip of the beak.

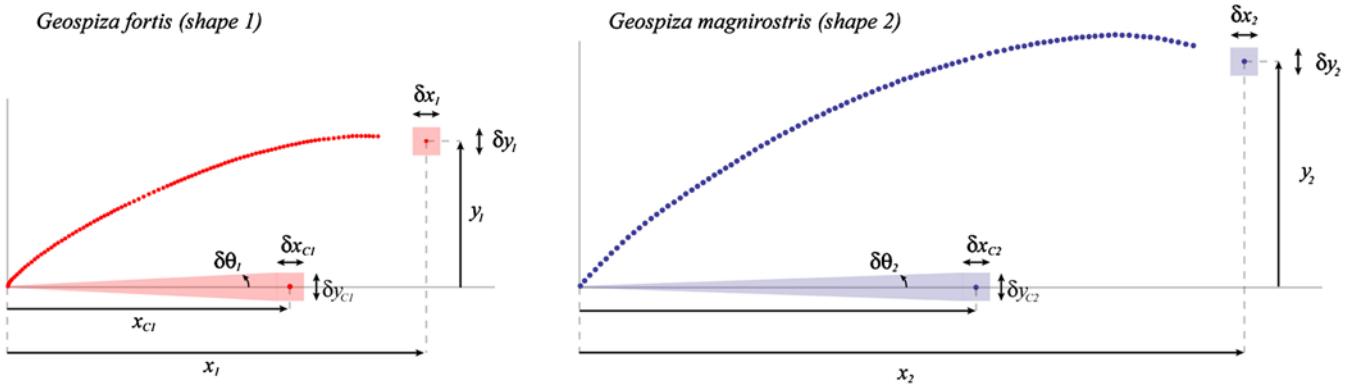

Fig. S2. Error sources. We define the error sources (experimental uncertainty) in the digitization of the beak profiles of the Medium and Large Ground Finches (*G. fortis* and *G. magnirostris* respectively), as they define the relevant range of scaling factors that may lead to the collapse of the shapes.

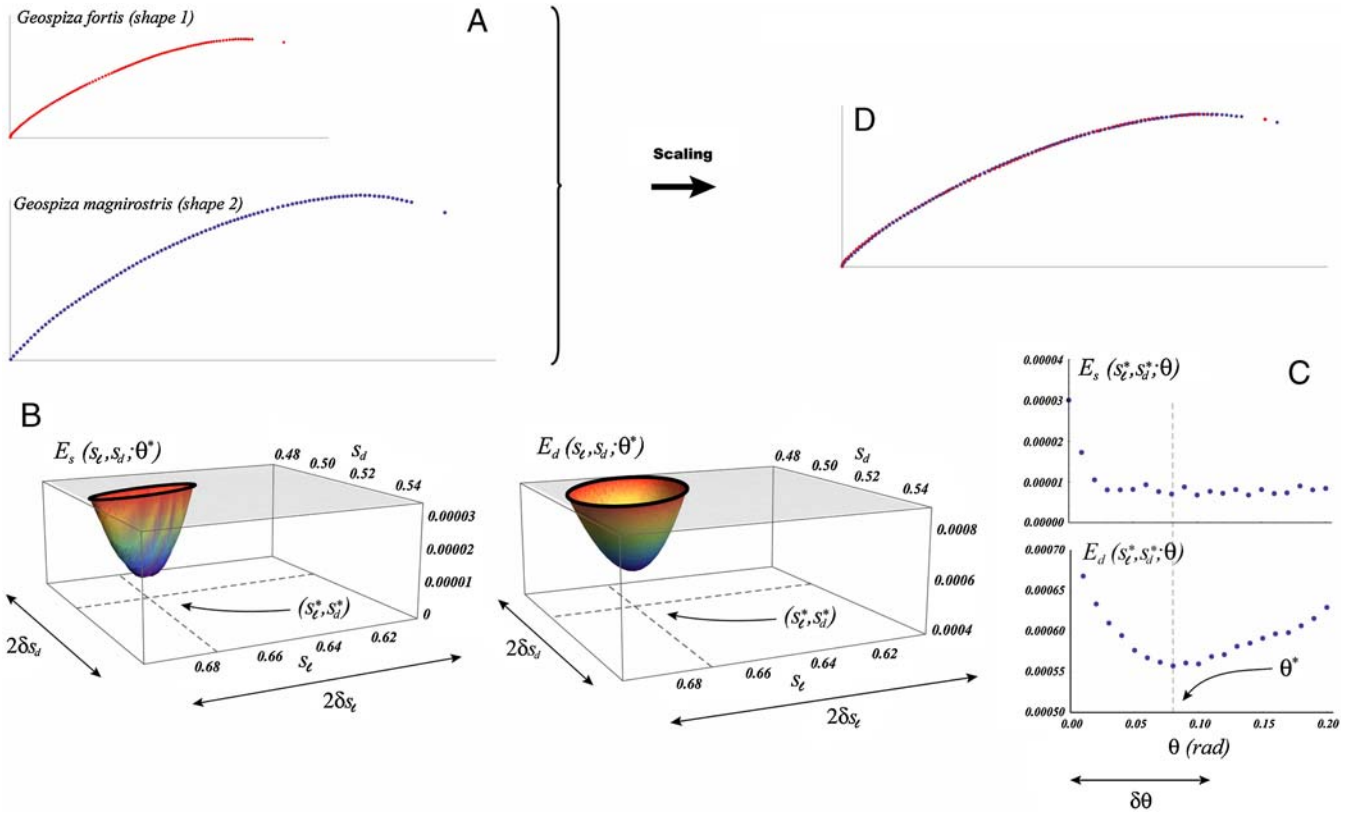

Fig. S3. Quantitative comparison of the upper beak shapes of Medium and Large Ground Finches. (*A*) Beak shapes of the Medium and Large Ground Finches used in the analysis. (*B*,*C*) We evaluate the measures E_s and E_d as a function of the angle θ and the scaling factors s_ℓ and s_d, within the range of these parameters that the experimental uncertainty allows for. We plot sections of the functions $E_s(s_\ell, s_d; \theta)$ and $E_d(s_\ell, s_d; \theta)$ for the optimal value of the angle θ^* to show the existence of a minimum in the (s_ℓ, s_d) subspace (*B*), and also for the optimal values of the scaling factors s_ℓ^* and s_d^* to show the existence of a minimum as a function of θ (*C*). Although the dependence of $E_s(s_\ell^*, s_d^*; \theta)$ on θ is not strong within a large range of values of θ, the measure $E_d(s_\ell^*, s_d^*; \theta)$ shows a clear minimum (*C*). (*D*) Collapsed shapes for the optimal values s_ℓ^*, s_d^* and θ^* obtained from minimization of the measures E_s and E_d.

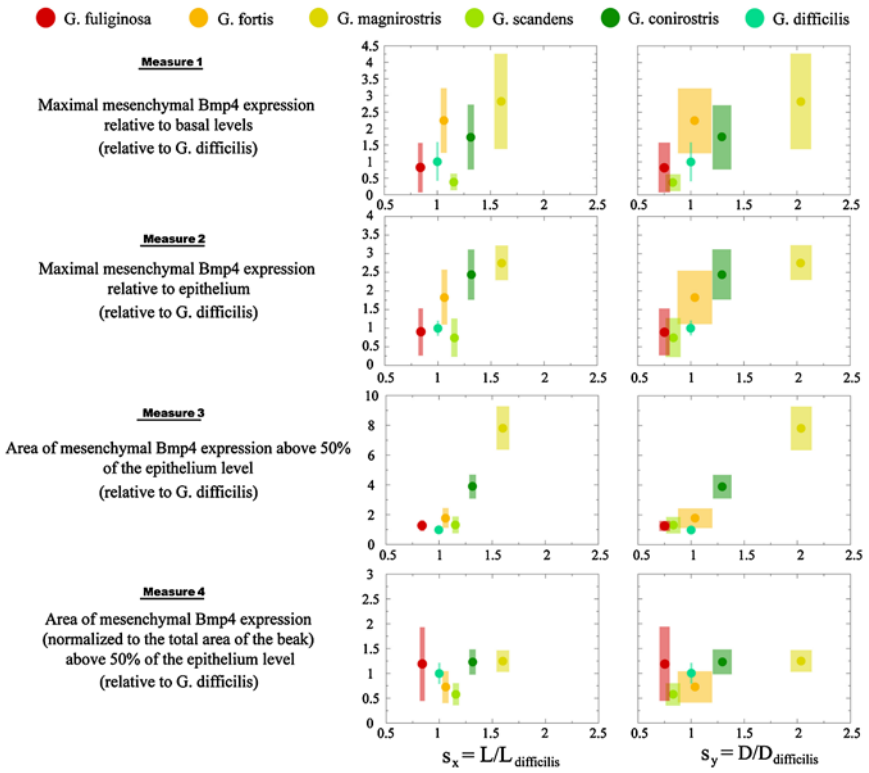

Fig. S4. Measures of mesenchymal *Bmp4* expression and correlation with adult beak morphology. (*Left*) Definition of the measure of *Bmp4* expression in midsaggital sections of the frontonasal mass for the diffent species in *Geospiza*. (*Right*) Plots of the measures of *Bmp4* expression defined as a function of the scaling factors that quantify adult beak morphological variability. Error bars in the different measures of *Bmp4* expression correspond to the standard deviation obtained from 3 specimens of each species.